Microchimica Acta (2020) 187: 84
https://doi.org/10.1007/s00604-019-4066-5

ORIGINAL PAPER

A terbium(III)-functionalized zinc(II)-organic framework for fluorometric determination of phosphate

Chuan Fan[1,2] · Xiaoxia Lv[2] · Meng Tian[1] · Qingcai Yu[1] · Yueyuan Mao[1] · Wanwei Qiu[1] · Hua Wang[2] · Guodong Liu[1,3]

Received: 5 July 2019 / Accepted: 6 December 2019 / Published online: 2 January 2020
© Springer-Verlag GmbH Austria, part of Springer Nature 2020

Abstract

A terbium(III)-functionalized zinc(II)-organic framework (Tb-MOF-Zn) is shown to be a viable fluorescent probe for phosphate. The organic ligands 4,4′,4″-[(2,4,6-trimethylbenzene-1,3,5-triyl)tris(methylene))tris(oxy)]tribenzoic acid (H_3L^3) contains multiple carboxyl groups that can react with zinc(II) to yield tubular MOF-Zn. The MOF-Zn was further functionalized with Tb(III) to produce a lanthanide composite of type Tb-MOF-Zn which displays strong fluorescence with excitation/emission maxima at 285/544 nm. Fluorescence is quenched by phosphate because of the specific interaction with Tb(III) in Tb-MOF-Zn. The concentration of Tb-MOF-Zn, reaction time and pH value of the solution were optimized. Fluorescence drops linearly in the 0.01 to 200.0 μM phosphate concentration range, and the detection limit is 4.0 nM. The fluorescent probe was also used to prepare a microdot array on a glass slide for visual detection of phosphate under illumination with UV light.

Keywords Rare earth · MOF · Fluorescence · Microdot array

Introduction

Phosphate ions are involved in many biological functions such as energy exchange, cellular signal transduction, and mineral metabolism. The level of phosphate ions in body fluid is used for the diagnosis of hyperparathyroidism and fanconisyndrome [1–3]. Phosphate as food preservatives and additives is applied to preserve meat, soft cheeses products and other different food products. Excessive intake of phosphate is harmful to blood vessels and accelerates aging [4]. The high level of phosphate in natural water such as reservoirs, lakes, estuaries, sea and rivers can result in severe environmental issues like eutrophication, which leads to a reduction of water quality [5]. Therefore, a reliable, sensitive and selective method for detecting phosphate is of great significance for the human health and environmental protection.

Various methods have been established for the quantitative analysis of phosphate ions, such as colorimetric analysis [6], fluorescence analysis [7–9], chromatography [10], electrochemical analysis [11], and enzymatic biosensors [12]. In particularly, fluorescent analysis has attracted considerable attention due to its extraordinary advantages such as high sensitivity, simple operation, and outstanding analysis performances and so on [13, 14]. However, selective and sensitive detection of phosphate ions in aqueous media is still a challenge because of the strong competitive solvation effect, requiring a strong affinity between recognition sites and phosphate [15]. Traditional molecular fluorescent probes are commonly used in homogeneous analysis systems, which encounter difficulties in separation and recovery in aqueous solution analysis [16]. In order to enhance the efficacy of fluorescence assay target objects, a lot of efforts have been made to design heterogeneous systems, including integrating molecular fluorescent probes into a support matrix [3].

Chuan Fan and Xiaoxia Lv are equal authors.

Electronic supplementary material The online version of this article (https://doi.org/10.1007/s00604-019-4066-5) contains supplementary material, which is available to authorized users.

✉ Hua Wang
huawangqfnu@126.com; http://wang.qfnu.edu.cn

✉ Guodong Liu
guodong.liu@ndsu.edu

[1] Research Center for Biomedical and Health Science, Anhui Science and Technology University, Fengyang 233100, China

[2] Institute of Medicine and Materials Applied Technologies, College of Chemistry and Chemical Engineering, Qufu Normal University, Qufu City, Shandong Province 273165, People's Republic of China

[3] Department of Chemistry and Biochemistry, North Dakota State University, Fargo, ND 58102, USA

It is known that fluorescent probes with short excited-state lifetimes are vulnerable to background interference, which severely limits its applications in complex matrixes and in vivo measurements [17]. Therefore, time-delayed fluorescent measurement using long life-time luminescent probes has evolved as a promising technique. In particularly, the trivalent lanthanide Ln(III)-based complexes possess a combination of several desirable properties for assay design: long excited state life-times, sharp line-like emissions and large Stokes shifts [18]. The use of visible-emitting Ln (III)-based systems in the design of targeting luminescent assay is particularly promising.

Metal organic frameworks (MOFs) which contain inorganic metal or metal oxide nodes and organic linkers have attracted a lot of attention. Based on many of its excellent properties (high porosity, big surface area, tunable structure and channels), MOFs have been widely used for gas storage and separation, catalysis, drug delivery, and biological assay [13, 19, 20]. More importantly, luminescent MOFs (LMOFs) have been successfully exploited as a unique assay platform [21–23]. Intrinsic porosity and functional groups of LMOFs promote preferred analyte binding and pre-concentrate the guest molecules in the network, benefitting to the selective and sensitive detection. For instance, Huang and co-workers has reported a simple method for phosphate detection by developing an off-on fluorescence probe of europium-adjusted carbon dots, which have been successfully applied to the detection of phosphate in complicated matrixes [7]. A displacement assay with a dimeric lanthanide luminescent ternary Tb(III)-cyclen complex was reported for the detection of phosphate ions with high selectivity [24].

Herein, we report a terbium functionalized metal-organic frameworks of zinc (Tb-MOF-Zn) as fluorescent probe for the detection of phosphate ions with high selectivity and sensitivity.

Experimental

Chemicals and reagents

1,3,5-Trimethylbenzene, methyl para-hydroxybenzoates, anhydrous potassium carbonate, paraformaldehyde, sodium hydroxide, acetone, zinc nitrate hexahydrate, terbium trichloride hexahydrate, and sodium phosphate were purchased from the Aladdin reagent Co., Ltd. (https://www.aladdin-e.com/). The hydrobromic acid (30% acetic acid solutions) was got from the J&K Scientific Ltd. (http://www.jkchemical.com/). All chemicals were of analytical grade, and all glass containers were cleaned by aqua regia and ultrapure water.

Apparatus

The fluorescence measurements were conducted by using fluorescence spectrophotometer (Hitachi, F-4600, Japan, http://www.hitachi.com.cn/) operated at an excitation wavelength of 285 nm, with both excitation and emission slit widths of 5.0 nm and voltage 700 V. The MOF materials were characterized with transmission electron microscope (TEM, JEM-2100, Japan, http://www.jeol.com.cn/), energy dispersive spectroscopy (EDS, Zeiss EVO®18), and field-emission scanning electron microscopy (SEM, Zeiss EVO®18, http://www.zeiss.com.cn/). UV-1510 (Thermo Fisher Multiskan™, https://www.thermofisher.com/cn/zh/home.html) was used to obtain the UV − vis spectra of MOF-Zn, Tb-MOF-Zn, Tb-MOF-Zn in the presence of phosphate, and MOF-Zn in the presence of phosphate.

Synthesis of the organic ligands of 4,4′,4″-(((2,4,6-trimethylbenzene-1,3,5-triyl) tris(methylene))tris(oxy))tribenzoic acid (H_3L^3)

1,3,5-Tribromomethyl-2,4,6-trimethylbenzene was prepared with previously reported methods [25]. Then 11.88 g (30 mmol) of the 1,3,5-tribromomethyl-2,4,6-trimethylbenzene and 13.82 g of anhydrous potassium carbonate (100 mmol) and 15.2 g of methyl parahydroxybenzoats (100 mmol) were added into the round bottom flask. And then 200 mL of treated acetone was added with continuous stirred and refluxed for 6 h. Next, filtered with hot and cooled to room temperature and then a white precipitate appeared. Then the intermediate products of ester were obtained by filtration, washed three times with water and dried in vacuum at 60 °C. The intermediate products were added to the flask, and a methanol solution with sodium hydroxide was added and then the mixture was refluxed for 12 h. Finally, the products were cooled to room temperature, and adjusted to the pH of about 2 with concentrated hydrochloric acid. The white precipitate appeared, which was filtered, washed three times with water, and dried in vacuum at 60 °C.

Preparation of MOF-Zn

The H_3L^3 (0.08556 g, 0.15 mmol) and $ZnNO_3 \cdot 6H_2O$ (0.06694 g, 0.225 mmol) were dissolved in 12 mL of DMF/H_2O (*V*/V: 2/1)) and stirred for 20 min. The mixture was transferred to a stainless steel reactor with a Teflon-lined and heated to 100 °C, and the reaction was proceeded for 72 h. Finally, the reactor was cooled to room temperature, and the solution was filtered. The product was washed three times with DMF to get colorless columnar crystals materials.

Preparation of Tb-MOF-Zn

MOF-Zn (0.1 mg) was added to 24 mL of the deionized water and dispersed uniformly by ultrasound. Then under the stirring condition, the aqueous solutions of $TbCl_3 \cdot 6H_2O$ (10 mM, 200 μL) were added at room temperature with reaction for

5 min, and then the yielded products of Tb-MOF-Zn were centrifuged (8000 rpm, 10 min) and washed three times with deionized water, and then be stored at 4 °C for future usage.

Fluorometric determination of phosphate with Tb-MOF-Zn composites

The selective detections of phosphate ions were conducted by the following procedure. First, the Tb-MOF-Zn composites (2.66 μg mL^{-1}) were dispersed in deionized water. Then, phosphate ions with different concentration was added and the mixture was incubated 20 min at room temperature. Fluorescene spectra of Tb-MOF-Zn were measured before and after addition of phosphate ions. The quenching efficiencies of Tb-MOF-Zn composites were calculated according to the equation: quenching efficiencies = $(F_0 - F)/F_0$, where F_0 and F refer to the fluorescence intensities of Tb-MOF-Zn composites (λ_{ex} = 285 nm, λ_{em} = 488 nm, 544 nm) in the absence and presence of anion ions, respectively. Specificity of fluorescent assay phosphate ions was studied by testing the responses of common anion ions (10 μM) including CO_3^{2-}, SO_4^{2-}, HCO_3^{2-}, CH_3COO^-, $C_5H_7O_5COO^{3-}$, $C_2O_4^{2-}$, Cl^-, and NO_3^- ions.

Preparation of the Tb-MOF-Zn composite microdot array

Tb-MOF-Zn composites were dispersed in deionized water and then an aliquot of 0.5 μL of Tb-MOF-Zn composites was spotted onto the cleaned glass plate surface and dried in the dark. The Tb-MOF-Zn composites microdot arrays were kept in the dark at 4 °C for future usage.

Results and discussion

Preparation and characterization of Tb-MOF-Zn composites

Scheme 1 llustrates the procedure of preparing Tb-MOF-Zn and the principle of fluorescent assay of phosphate. 1,3,5-tribromomethyl-2,4,6-trimethylbenzene was used a precursor to prepare a flexible polycarboxylic ligand of 4,4′,4″-(((2,4,6-trimethylbenzene-1,3,5-triyl)tris(methylene))tris(oxy))tribenzoic acid (H_3L^3) by introducing a flexible group -CH_2O- between the central benzene ring and benzoic acid. Carboxyl groups of H_3L^3 were used as connect units to coordinate with zinc ions under the hydrothermal reaction conditions, forming MOF-Zn. Furthermore, the terbium (Tb^{3+}) ions were introduced to react with MOF-Zn to yield the lanthanide composites (Tb-MOF-Zn) with strong fluorescence. The fluorescence intensity of the Tb-MOF-Zn composites is significantly quenched in the presence of phosphate ions due to the specific interaction between Tb^{3+} and phosphate ions.

Scanning electron microscope (SEM), transmission electron microscope (TEM), energy dispersive spectroscopy (EDS), fluorescent spectra and UV − vis spectra were used to characterize the Tb-MOF-Zn and confirm the principle of

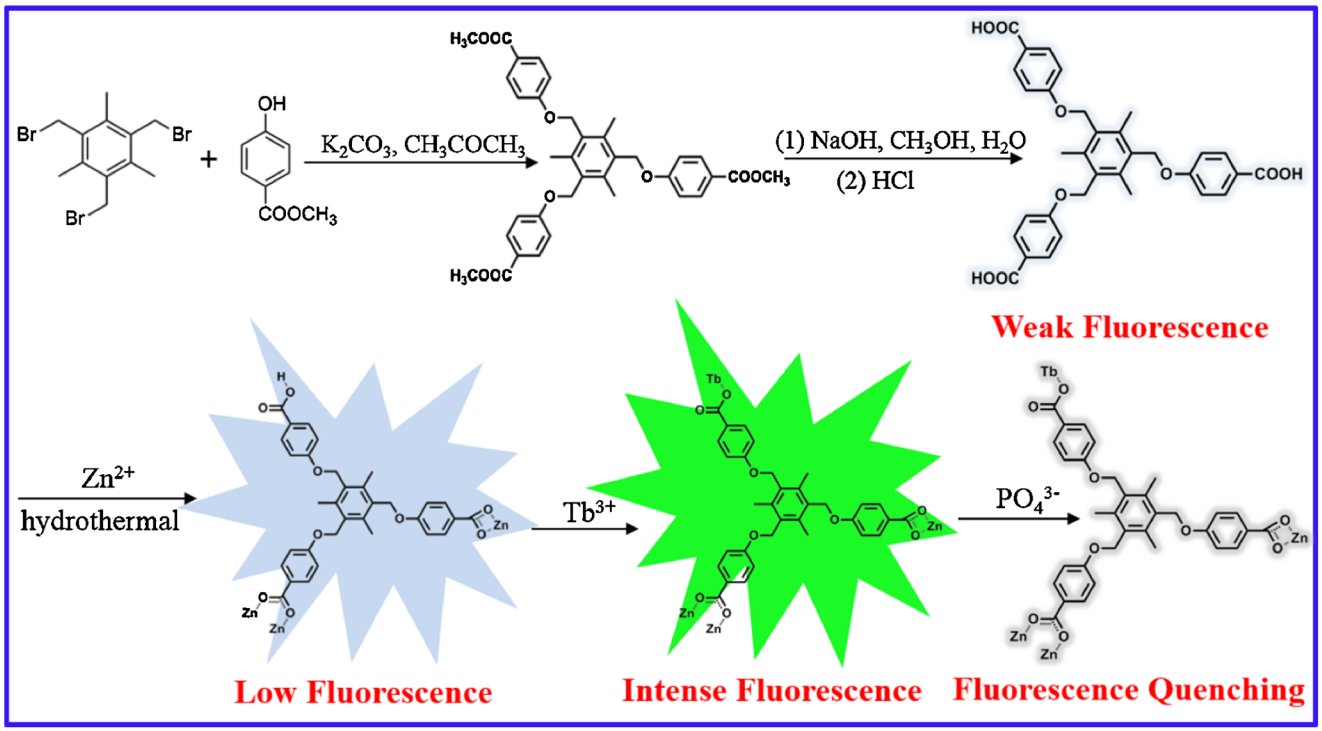

Scheme 1 Schematic illustration of preparing Tb-MOF-Zn composite and the principle of fluorescent assay of phosphate.

fluorescent assay phosphate ions. Fig. 1a presents the typical SEM image of MOF-Zn. One can see that the MOF-Zn has a tubular structure with the length ranging from 2 to 10 μm. The diameter of tubular MOF-Zn is around 420 nm (Fig. 1b). It is noted that a similar morphology of the Tb-MOF-Zn was observed after introducing Tb^{3+} ions to MOF-Zn (Fig. 1c). Figure 1d to f present the SEM images of T-MOF-Zn in the presence of different concentrations of phosphate. When 1 mM of phosphate ions was added, most the Tb-MOF-Zn composites can maintain the original structure (Fig. 1d); however, when the concentrations of phosphate ions increased from 2 to 4 mM, the Tb-MOF-Zn structure begins to collapse (Fig. 1e) until it's completely decomposed (Fig. 1f). This result was consistent with the previous report that phosphate ions would damage their structures according to the coordination of zinc atoms in MOFs with phosphate ions [26]. In addition, EDS was also applied to explore the morphological structure and chemical composition of MOF-Zn (Figure S1) and Tb-MOF-Zn (Figure S2). The tubular structures were observed on the EDSs of both MOF-Zn and Tb-MOF-Zn (inserts). The elemental profile of MOF-Zn shows that zinc ions were linked with the MOF successfully (Figure S1); and the elemental profile of Tb-MOF-Zn indicates that Tb was introduced to MOF-Zn (Figure S2). Moreover, the XRD is studied as shown in Figure S3. The date revealed the typical peak of MOF-Zn, but the intensity of Tb-MOF-Zn was too low.

Figure 2a presents the fluorescence spectra of MOF-Zn, Tb-MOF-Zn and Tb-MOF-Zn in the presence of 1 mM of phosphate ions. One can see that Tb-MOF-Zn exhibits two characteristic emission peaks of Tb at 488 nm and 544 nm (red curve), and MOF-Zn doesn't have emission peak at the same range of wavelength (purple curve on the bottom). This result also confirms that Tb was introduced to MOF-Zn successfully and the produced lanthanide composites (Tb-MOF-Zn) has strong fluorescence. The photoluminescence spectra exhibit characteristic emission peaks at about 488, and 544 nm due to the f − f transitions of the Tb^{3+} ions ($^5D_4 - {}^7F_6$, $^5D_4 - {}^7F_5$), which are attributed to the antenna effect that stems from energy transfer from the ligand to the Tb^{3+} ions [27]. It is noted that the fluorescence

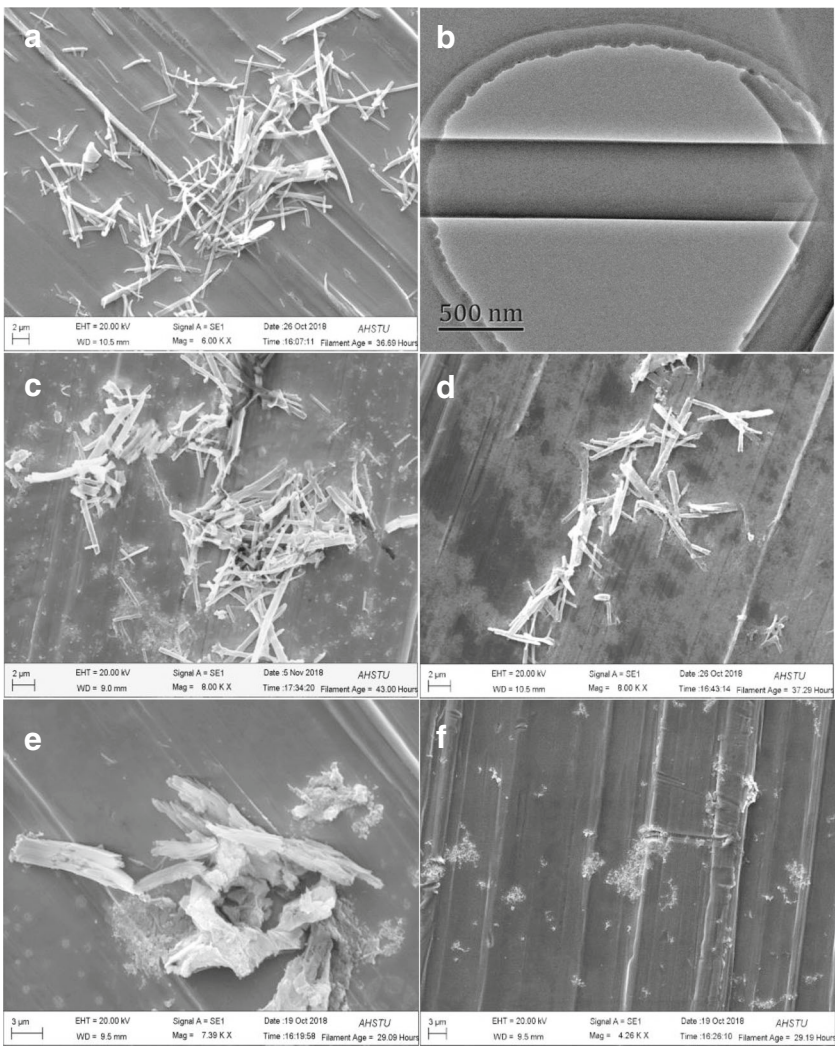

Fig. 1 **a** SEM images of MOF-Zn; **b** TEM image of MOF-Zn; **c** SEM image of Tb-MOF-Zn; **d** SEM image of Tb-MOF-Zn in the presence of 1 mM of phosphate ions; **e** SEM image of Tb-MOF-Zn in the presence of 2 mM of phosphate ions; and (**f**) SEM image of Tb-MOF-Zn in the presence of 4 mM of phosphate

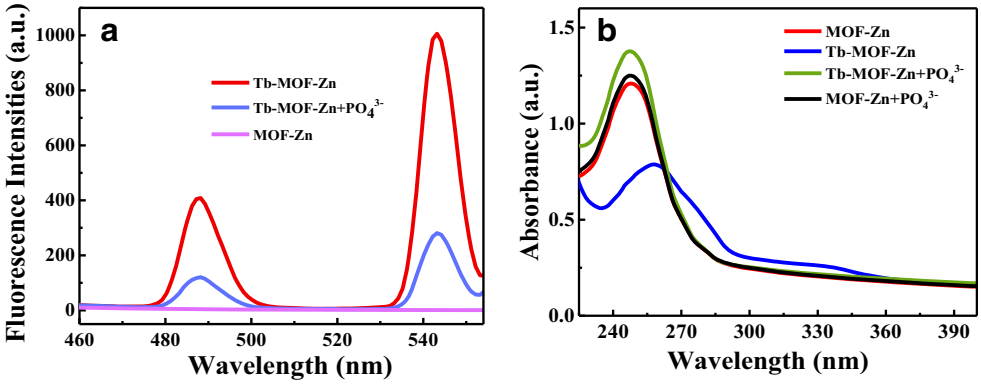

Fig. 2 **a** Fluorescence spectra of MOF-Zn, Tb-MOF-Zn, and Tb-MOF-Zn in the presence of 10 μM of phosphate. Excitation wavelength: 285 nm; **b** UV − vis spectra of MOF-Zn (red), Tb-MOF-Zn (blue), Tb-MOF-Zn in the presence of 10 μM of phosphate (green), and MOF-Zn in the presence of 10 μM of phosphate (black)

intensity of the Tb-MOF-Zn composites was quenched in the presence of phosphate ions (blue curve). To confirm the principle of fluorescent assay phosphate ions with Tb-MOF-Zn composite, we compared the UV − vis absorption spectra of MOF-Zn, Tb-MOF-Zn, Tb-MOF-Zn in the presence of phosphate ions, and MOF-Zn in the presence of phosphate ions (Fig. 2b). One can see that MOF-Zn displays an absorption peak at about 248 nm (red curve) and there is no obvious change on the wavelength and intensity of absorption peak in the presence of phosphate ions (black curve), indicating there is negligible interaction between MOF-Zn and phosphate ions. The absorption peak of Tb-MOF-Zn shifts to 258 nm and the intensity of the peak decreases around 50% (blue curve). The results indicate that the Tb^{3+} ions might bind with the uncoordinated carboxyl functional groups of MOF-Zn leading to the noticeable shift of the UV-vis absorption peak, which is consistent with the previous reports [28, 29]. In the presence of phosphate ions, the absorption peak of Tb-MOF-Zn shifts back to 248 nm and the intensity of the absorption peak recovers to the level of MOF-Zn (green curve). The above results show that phosphate ions has strong binding ability with the Tb^{3+} ions to produce the lanthanum–phosphate complex [30].

Selectivity of the fluorometric assay for phosphate with Tb-MOF-Zn composites Selectivity of fluorescent assay of phosphate with Tb-MOF-Zn was studied by examing the fluorescence response of Tb-MOF-Zn suspension in the presence of various anions, such as CO_3^{2-}, SO_4^{2-}, HCO_3^-, CH_3COO^-, $C_5H_7O_5COO^{3-}$, $C_2O_4^{2-}$, Cl^-, and NO_3^-. Figure 3a illustrates that the quenching efficiency of various anions to the fluorescence of Tb-MOF-Zn suspension. As expected, no obvious fluorescence quenching were observed for the common anions in the suspension except phosphate ions, only phosphate ions triggered the quenching of fluorescence emissions of Tb-MOF-Zn, evidencing the special recognition capability of Tb-MOF-Zn to phosphate ions in aqueous solution. Figure 3b presents the quenching effect of phosphate ions on the fluorescence of Tb-MOF-Zn in the presence of other anions. There is no effect on the quenching effect of phosphate ions when other anions coexisted. The results indicate that this MOF is a robust fluorescent probe for the selective detection of phosphate. It has high selectivity over other anions.

Optimization of experimental parameters for fluorometric assay To obtain the best performance of fluorescent assay of phosphate with Tb-MOF-Zn composite, the following parameters were optimized, including (**A**) Tb-MOF-Zn concentration; (**B**) incubation time; (**C**) the pH value of solution. Respective detailed data and results are all given in the Supporting Information (Figure S4). And the following assay conditions were found to give the best assay performances: (**A**) Using 2.66 μg mL^{-1} Tb-MOF-Zn composite; (**B**) Using

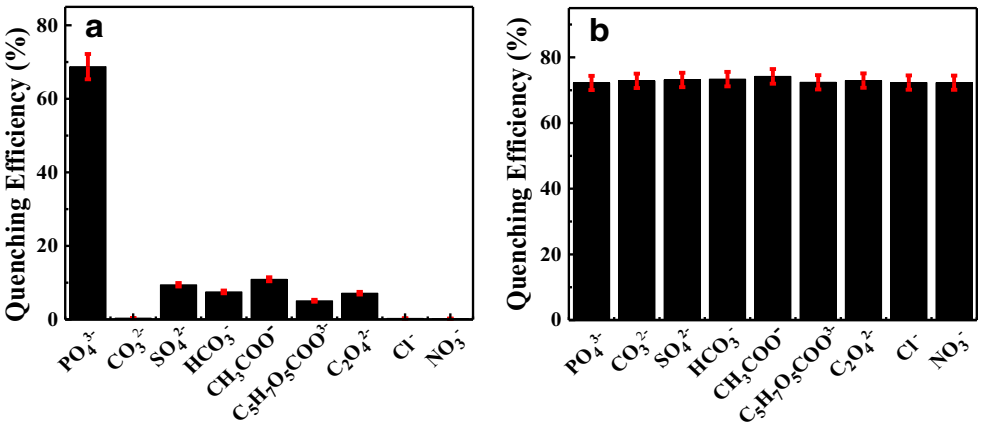

Fig. 3 The quenching efficiency of the Tb-MOF-Zn towards various anions (**a**) with phosphate, CO_3^{2-}, SO_4^{2-}, HCO_3^{2-}, CH_3COO^-, $C_5H_7O_5COO^{3-}$, $C_2O_4^{2-}$, Cl^-, and NO_3^- (10 μM); **b** The quenching efficiency of the Tb-MOF-Zn in the presence of different anions co-existing with phosphate (λ_{ex} = 285 nm, λ_{em} = 544 nm)

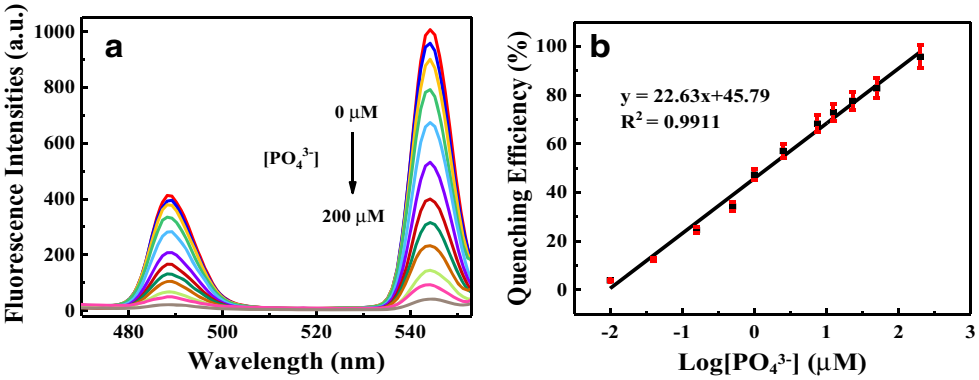

Fig. 4 **a** The fluorescence response of a Tb-MOF-Zn suspension upon the addition of various concentrations of phosphate ions under the excitation at 285 nm; **b** standard calibration plot for the relationships between the quenching efficiency and the logarithm of phosphate ions concentrations

20 min as incubation time; (**C**) Using pH 7.0 to prepare the sample solutions. In addition, the reproducibility of the assay was evaluated by running the assay in the presence of 0.01 μM, 1 μM, 100 μM phosphate ions. The relative standard deviation (RSD) at 0.01 μM, 1 μM, 100 μM were calculated to be 4%, 3%, and 1%, respectively (Figure S5). Furthermore, the photostability of Tb-MOF-Zn was investigated (Figure S6). The results validate that the Tb-MOF-Zn can exhibit good stability even at room temperature.

Analytical performance of the assay Under the optimal conditions, sample solutions with different concentrations of phosphate ions were tested with Tb-MOF-Zn composites. Figure 4a shows the fluorescence spectrums of Tb-MOF-Zn in the presence of different concentrations of phosphate ions. One can see the fluorescence intensities of Tb-MOF-Zn at both 488 nm and 544 nm decrease with the increase of the concentrations of phosphate ions. Due to the high fluorescence intensity of Tb-MOF-Zn at 544 nm, we choose the emission peak at 544 nm to quantify the concentration of phosphate ions. The resulting calibration plot (Fig. 4b) of the logarithm of phosphate ions concentrations versus the quenching efficiency had a dynamic range from 0.01 to 200.0 μM ($R^2 = 0.9911$), and the limit of detection is 4 nM ($S/N = 3$). Table S1 summarizes the linear ranges and detection limits of phosphate ion detection based on different strategies and materials. One can see the Tb-MOF-Zn composite based fluorescent assay has a wider linear range and lower detection limit. Therefore, the method is specific for phosphate and showed excellent sensitivity.

Microdot array for visual detection of phosphate ions under UV light Due to the size of the Tb-MOF-Zn composites, its application to analysis of phosphate ions in the solution may affect accuracy, so we try to fix it on the glass plate for testing. Tb-MOF-Zn composites were used to prepare a microdot array for visual detection of phosphate ions under a UV light. Briefly, 0.5 μL of Tb-MOF-Zn suspension was spotted onto a cleaned glass slide, dried at room temperature. One microlitter of sample solution containing different concentrations of phosphate ions was applied to the microdot. Figure 5 displays the typical photo image of the microdot array after applying the sample solution with different concentrations. The microdot array includes triplet dots for each concentration. The concentrations of phosphate ions applied to the array were 0, 1, 10, 20, 40, 80, 100, 200 μM (from left to right), respectively. It can be seen that the fluorescence intensities of the microdots decreases with the increase of the concentration of phosphate ions. The threshold of visual detection is 10 μM.

Conclusions

The lanthanide composite Tb-MOF-Zn was synthesized and used as a viable fluorescent probe for the detection of phosphate with high selectivity and sensitivity. Under the optimal conditions, 10 μM of the phosphate can be visually detected under UV light. Thus, the established fluorescent strategy holds enormous potential for the simple, fast and sensitive detection of phosphates in aqueous media. Future work will aim to detect phosphate in complex environmental matrixes and biological fluids. More importantly, current work paves a pathway to design and synthesize functionalized MOF materials for detection of various analytes and expands the applications of MOFs in the fields of chemical and biomedical applications.

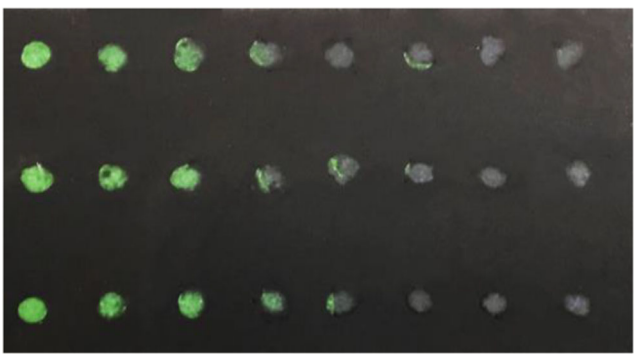

Fig. 5 Photo image of microdot array after applying the sample solutions with different concentrations of phosphate ions. Concentrations of phosphate ions (from left to side): 0, 1, 10, 20, 40, 80, 100, 200 μM

Acknowledgements This work is financially supported by the Wanjiang scholars in Anhui Province, China and the Institute of Health, Centers of Biomedical Research Excellence (NIH, COBRE, Grant number: P20 GM109024). Its contents are solely the responsibility of the authors, and do not necessarily represent the official views of the NIH.

Compliance with ethical standards

Conflict of interest The author(s) declare that they have no conflict of interest.

References

1. Cheng WL, Sue JW, Chen WC, Chang JL, Zen JM (2010) Activated nickel platform for electrochemical sensing of phosphate. Anal Chem 82:1157–1161
2. Wygladacz K, Qin Y, Wroblewski W, Bakker E (2008) Phosphate-selective fluorescent sensing microspheres based on uranyl salophene ionophores. Anal Chim Acta 614:77–84
3. Yang J, Dai Y, Zhu X, Wang Z, Li Y, Zhuang Q, Shi J, Gu J (2015) Metal-organic frameworks with inherent recognition sites for selective phosphate sensing through their coordination-induced fluorescence enhancement effect. J Mater Chem A 3:7445–7452
4. Ahmad R, Ahn MS, Hahn YB (2017) ZnO nanorods array based field-effect transistor biosensor for phosphate detection. J Colloid Interface Sci 498:292–297
5. Mak WC, Chan C, Barford J, Renneberg R (2003) Biosensor for rapid phosphate monitoring in a sequencing batch reactor (SBR) system. Biosens Bioelectron 19:233–237
6. Liu W, Du Z, Qian Y, Li F (2013) A specific colorimetric probe for phosphate detection based on anti-aggregation of gold nanoparticles. Sensors Actuators B Chem 176:927–931
7. Zhao HX, Liu LQ, Liu ZD, Wang Y, Zhao XJ, Huang CZ (2011) Highly selective detection of phosphate in very complicated matrixes with an off-on fluorescent probe of europium-adjusted carbon dots. Chem Commun 47:2604–2606
8. Ganjali MR, Hosseini M, Memari Z, Faridbod F, Norouzi P, Goldooz H, Badiei A (2011) Selective recognition of monohydrogen phosphate by fluorescence enhancement of a new cerium complex. Anal Chim Acta 708:107–110
9. Spangler C, Schaeferling M, Wolfbeis OS (2008) Fluorescent probes for microdetermination of inorganic phosphates and biophosphates. Microchim Acta 161:1–39
10. Colina M, Gardiner PHE (1999) Simultaneous determination of total nitrogen, phosphorus and Sulphur by means of microwave digestion and ion chromatography. J Chromatogr A 847:285–290
11. Cinti S, Talarico D, Palleschi G, Moscone D, Arduini F (2016) Novel reagentless paper-based screen-printed electrochemical sensor to detect phosphate. Anal Chim Acta 919:78–84
12. Gilbert L, Jenkins ATA, Browning S, Hart JP (2011) Development of an amperometric, screen-printed, single-enzyme phosphate ion biosensor and its application to the analysis of biomedical and environmental samples. Sensors Actuators B Chem 160:1322–1327
13. Feng L, Liu M, Liu H, Fan C, Cai Y, Chen L, Zhao M, Chu S, Wang H (2018) High-throughput and sensitive fluorimetric strategy for microRNAs in blood using wettable microwells array and silver nanoclusters with red fluorescence enhanced by metal organic frameworks. ACS Appl Mater Interfaces 10:23647–23656
14. Yang ZC, Wang M, Yong AM, Wong SY, Zhang XH, Tan H, Chang AY, Li X, Wang J (2011) Intrinsically fluorescent carbon dots with tunable emission derived from hydrothermal treatment of glucose in the presence of monopotassium phosphate. Chem Commun 47:11615–11617
15. Beer PD, Gale PA (2001) Anion recognition and sensing: the state of the art and future perspectives. Angew Chem Int Ed 40:486–516
16. Khatua S, Choi SH, Lee J, Kim K, Do Y, Churchill DG (2009) Aqueous fluorometric and colorimetric sensing of phosphate ions by a fluorescent dinuclear zinc complex. Inorg Chem 48:2993–2999
17. Li J, Zhou W, Ouyang X, Yu H, Yang R, Tan W, Yuan J (2011) Design of a room-temperature phosphorescence-based molecular beacon for highly sensitive detection of nucleic acids in biological fluids. Anal Chem 83:1356–1362
18. Binnemans K (2009) Lanthanide-based luminescent hybrid materials. Chem Rev 109:4283–4374
19. Bobbitt NS, Mendonca ML, Howarth AJ, Islamoglu T, Hupp JT, Farha OK, Snurr RQ (2017) Metal-organic frameworks for the removal of toxic industrial chemicals and chemical warfare agents. Chem Soc Rev 46:3357–3385
20. Fan C, Lv X, Liu F, Feng L, Liu M, Cai Y, Liu H, Wang J, Yang Y, Wang H (2018) Silver nanoclusters encapsulated into metal-organic frameworks with enhanced fluorescence and specific ion accumulation toward the microdot array-based fluorimetric analysis of copper in blood. Acs Sensors 3:441–450
21. Dou Z, Yu J, Cui Y, Yu Y, Wang Z, Yang D, Qian G (2014) Luminescent metal–organic framework films as highly sensitive and fast-response oxygen sensors. J Am Chem Soc 136:5527–5530
22. Xiang Z, Fang C, Leng S, Cao D (2014) An amino group functionalized metal-organic framework as a luminescent probe for highly selective sensing of Fe^{3+} ions. J Mater Chem A 2:7662–7665
23. Wang GY, Song C, Kong DM, Ruan WJ, Chang Z, Li Y (2014) Two luminescent metal-organic frameworks for the sensing of nitroaromatic explosives and DNA strands. J Mater Chem A 2:2213–2220
24. Caffrey DF, Gunnlaugsson T (2014) Displacement assay detection by a dimeric lanthanide luminescent ternary Tb(III)-cyclen complex: high selectivity for phosphate and nitrate anions. Dalton Trans 43:17964–17970
25. Made AWVD, Made RHVD (1993) ChemInform abstract: a convenient procedure for bromomethylation of aromatic compounds. Selective mono-, Bis-, or Trisbromomethylation. Cheminform 58: 1262–1263
26. Ojida A, Nonaka H, Miyahara Y, Tamaru S, Sada K, Hamachi I (2006) Bis(Dpa-Zn(II)) appended xanthone: excitation ratiometric chemosensor for phosphate anions. Angew Chem Int Ed 45:5518–5521
27. Guanfeng J, Gao X, Zheng T, Weihua G, Houting L, Zhiliang L (2018) Postsynthetic metalation metal–organic framework as a fluorescent probe for the ultrasensitive and reversible detection of PO_4^{3-} ions. Inorg Chem 57:10525–10532
28. Daiguebonne C, Kerbellec N, Guillou O, Bünzli JC, Gumy F, Catala L, Mallah T, Audebrand N, Gérault Y, Bernot K (2008) Structural and luminescent properties of micro- and nanosized particles of lanthanide terephthalate coordination polymers. Inorg Chem 47:3700–3708
29. Kerbellec N, Kustaryono D, Haquin V, Etienne M, Daiguebonne C, Guillou O (2009) An unprecedented family of lanthanide-containing coordination polymers with highly tunable emission properties. Inorg Chem 48:2837–2843
30. Kim M, Kim H, Byeon SH (2017) Layered yttrium hydroxide l-Y(OH)3 luminescent adsorbent for detection and recovery of phosphate from water over a wide pH range. ACS Appl Mater Interfaces 9:40461–40470

Publisher's note Springer Nature remains neutral with regard to jurisdictional claims in published maps and institutional affiliations.